

C.P. No. 358

(19,054)

A.R.C. Technical Report

C.P. No. 358

(19,054)

A.R.C. Technical Report

LIBRARY
ROYAL AIRCRAFT ESTABLISHMENT
BEDFORD.



MINISTRY OF SUPPLY

AERONAUTICAL RESEARCH COUNCIL

CURRENT PAPERS

**Curves Suitable for Families of Aerofoils with
Variable Maximum Thickness Position, Nose
Radius, Camber and Nose Droop,**

By

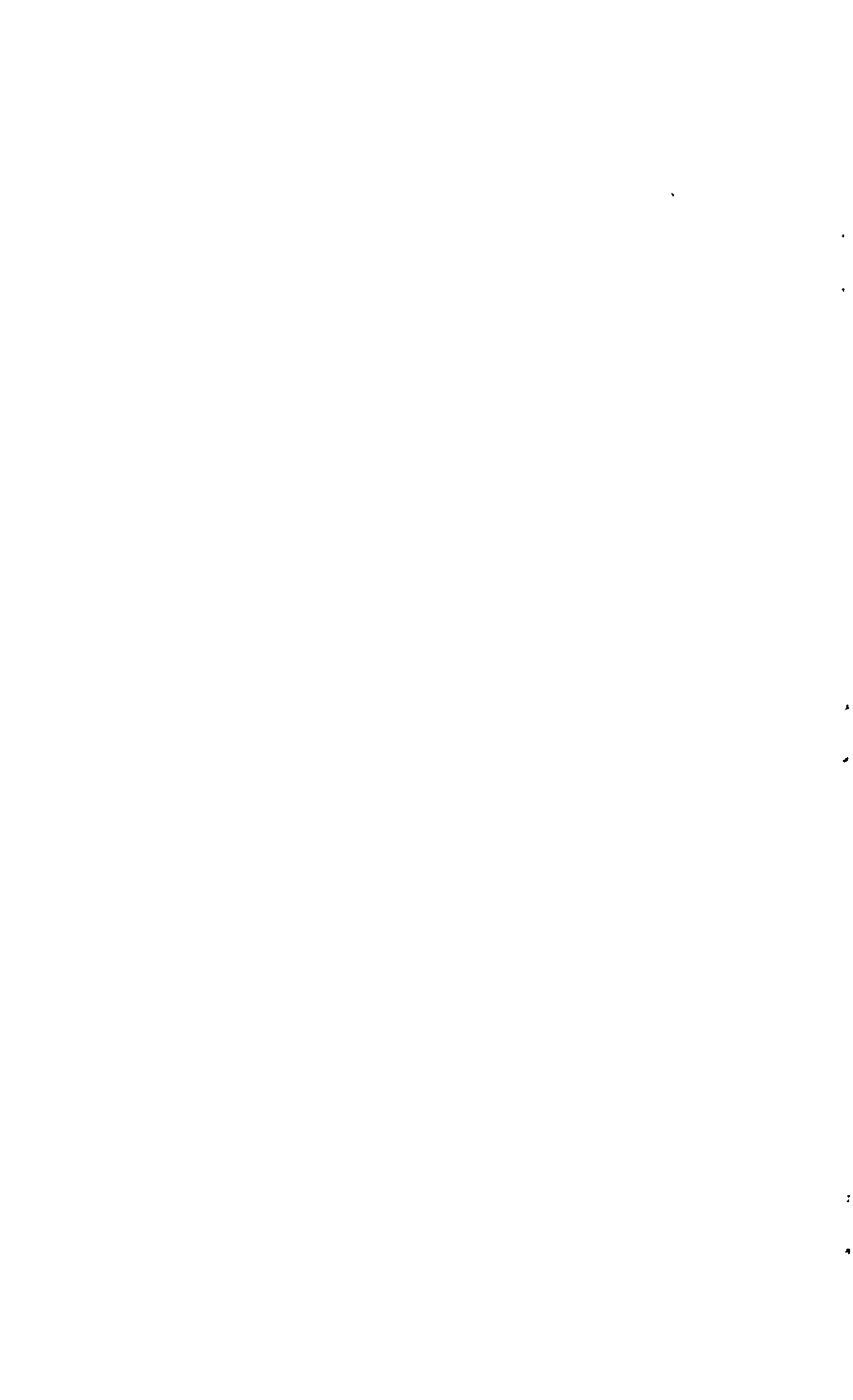
L. H. Tanner, B.A.,

of the Aerodynamics Division, N.P.L.

LONDON : HER MAJESTY'S STATIONERY OFFICE

1957

FOUR SHILLINGS NET



Curves Suitable for Families of Aerofoils with Variable
Maximum Thickness Position, Nose Radius,
Camber and Nose Droop

- By -

L. H. Tanner, B.A.,
of the Aerodynamics Division, N.P.L.

14th February, 1957

SUMMARY

The paper shows that it is possible to design geometric curves, given by single explicit equations, and having shapes suitable for use as aerofoil sections. A family of sharp-nosed sections with variable maximum thickness position is described. A method of rounding the leading edge of any sharp-nosed section is then suggested. Finally a family of curves with camber and nose droop is given. The methods used could be adapted to produce other section variations if required.

1. Introduction

In the design of an aerofoil section for high-speed aeroplanes, it is sometimes possible to specify the general characteristics, such as thickness, maximum thickness position and nose radius, which are required. The problem is then to design a smooth curve having these properties. This has sometimes been done by fitting together several algebraic curves, making sure that the ordinates and their first and possibly second derivatives are continuous at the join. This method is however unsatisfactory in several ways. The higher derivatives are often discontinuous and the curve not sufficiently smooth. It is difficult to vary one characteristic (e.g., nose radius or maximum thickness position) while leaving the general shape unchanged. The lack of a single explicit equation for the whole curve may lead to complication in calculating the low speed pressure distribution.

The present paper gives examples showing that it is possible to design geometrical curves, given by single explicit equations, which are suitable for aerofoil sections. The curves have all their derivatives continuous and their shape is given by parameters which enable nearly independent variation of maximum thickness position, nose radius, etc.

The first family of curves described was used by Michel, Marchaud and Le Gallo¹ for bump sections. They provide useful sharp-nosed aerofoil sections with variable maximum thickness position.

A method is then given for rounding the nose of these or any other sharp-nosed sections, and the resulting nose shapes are described in detail.

Finally/

Finally a method is given for adding an extended and drooped nose to these sections.

Apart from the value of the particular examples given, the methods shown will suggest possibilities for designing curves of any other shapes which may be required.

2. Notation

English symbols

A	=	$\alpha_1 x(1-x^{n_1}) + \alpha_2 x(1-x^{n_2})$,	Section 5.2
a		Length cut off in rounding the nose,	Section 4.2
B	=	$\alpha_1 x(1-x^{n_1}) - \alpha_2 x(1-x^{n_2})$,	Section 5.2
b		Intercept of linear portion under the drooped nose with the x-axis,	Section 5.2
C	=	$-L \log (e^{-B/L} + e^{-D/L})$,	Section 5.2
c	=	$\left(\frac{\alpha_1 + \alpha_2}{\alpha_1} \right)^{1/n}$,	Section 3.4
		Chord of sharp-nosed aerofoil with droop,	Section 5.2
D	=	$-m(x-b)$,	Section 5.2
E		Ordinate of droop-nosed aerofoil,	Section 5.2
L		Parameter in the fairing curve C,	Sections 5.2, 5.3
m		Slope of linear portion under the nose of the drooped aerofoil,	Section 5.2
N		Axis ratio of conic,	Section 4.3
n		Parameter determining maximum thickness position,	Section 3
t		Maximum thickness/chord ratio of aerofoil,	Section 3.2
x	}	Co-ordinates	
y			

Greek symbols

α		Parameter determining thickness,	Section 3
β		Parameter determining nose shape,	Section 4
γ		Ratio to the nose radius of the basic-section ordinate at $x = a + \rho$,	Section 4.4
ϵ	=	$\frac{x-a}{a}$,	Section 4.3

- η Ordinate, Sections 4, 5
- ρ Nose radius, Section 4
- $\phi = \frac{\eta_a}{a}$, Section 4.3
- ψ Slope of basic sharp-nosed section at $x = a$, Section 4.3
- δ Parameter determining thickness for $n = 0$, Section 3.1

3. A Family of Symmetrical Aerofoils¹

3.1 Equation and general properties

A family of curves suitable for sharp-nosed aerofoil sections is

$$y = \pm \alpha x [1-x^n] \quad \dots(3.1)$$

where $y = 0$ at $x = 0$ and at $x = 1$, so that the chord is unity.

The possible range of the parameter n , which determines the maximum thickness position, is from -1 to $+\infty$. The effect of this parameter is shown in Figs. 1, 2.

- For $n = -1$, the curve is triangular.
- For $-1 < n < -0.5$, the curve has an infinite slope and infinite radius of curvature at $x = 0$, e.g., Fig.1a.
- For $n = -0.5$, the curve has a finite radius equal to $\frac{1}{2}\alpha^2$ at $x = 0$, Fig.1b.
- For $-0.5 < n < 0$, the curve has infinite slope but zero radius at $x = 0$, e.g., Fig.1c.
- For $n = 0$, the limiting curve* $y = \delta x \log \frac{1}{x}$ is an approximation to an equiangular spiral, Fig.1d.
- For $n > 0$, the curve has a finite slope equal to α at $x = 0$, Fig. 2.

For all values of n the slope at $x = 1$ is $-\alpha n$. The slope at any value of x is:-

$$\frac{dy}{dx} = \alpha [1-(n+1)x^n] \quad \dots(3.2)$$

This is zero when $x = \left(\frac{1}{n+1}\right)^{1/n}$, so the maximum thickness position

is at this value of x . Fig. 3 shows a graph of the maximum thickness position against n . For $n = 1$ the curve is the parabolic arc having its maximum thickness at $x = 0.5$. For $n < 1$ the maximum thickness occurs at $x < 0.5$, whereas for $n > 1$ it occurs at $x > 0.5$. Hence if the curves with $n > 1$ are used for aerofoils and if their maximum thickness position is to be forward of 0.5, the curves must be reversed, so that x is zero at the trailing edge and unity at the leading edge.

Thus/

*Letting $\alpha \rightarrow \infty$ as $n \rightarrow 0$ so that the thickness remains finite.

Thus for any maximum thickness position other than 0.5 there are two possible curves, one with $n < 1$ and the other with $n > 1$. Fig. 1 shows, however, that negative values of n lead to unsuitable nose shapes, and so practically the range over which there are two possible sections is that of maximum thickness positions from $e^{-1} (= 0.368)$ to 0.5.

Fig. 4a shows, for comparison, the sections $n = 0$ and $n = 3$, which have approximately the same maximum thickness position, (37%), when one is reversed. This shows that the section with $n > 1$ is thinner and less curved, both at the leading and trailing edges. The curvature near the maximum thickness position is of course correspondingly greater.

3.2 Leading and trailing-edge slopes

From equation (3.2), for $n > 0$, the slopes at $x = 0$ and $x = 1$ are respectively α and $-\alpha n$. Thus if $n > 1$ the leading-edge slope is n times the trailing-edge slope, while if $n < 1$ it is $1/n$ times the trailing-edge slope (for aerofoils with their maximum thickness forward of mid-chord). The maximum thickness of the section is:-

$$t = 2\alpha \left(\frac{1}{n+1} \right)^{1/n} \frac{n}{n+1} \quad \dots(3.3)$$

Hence in terms of the thickness, α is given by:-

$$\alpha = \frac{t}{2n} (n+1)^{n+1/n}$$

Fig. 5 shows α and αn plotted against n , for $t = 0.10$. The trailing-edge slopes of the RAE 100-104 series² are also shown, at the values of n giving the same maximum thickness positions. This shows that the sections with $n > 1$ have nearly the same trailing-edge angles as the corresponding RAE sections, (within 7%), while the sections with $n < 1$ have trailing-edge angles 20 to 30% greater than the RAE sections.

Fig. 4b shows a comparison of the section $n = 2$ and the RAE 104 section, with the same chord and thickness. The maximum thickness position is nearly the same, and the sections differ little behind this position, except that the RAE section has a slight bump at about $x = 0.6$.

3.3 Curvature

When the slope, $\alpha [1-(n+1)x^n]$, is small, the curvature is approximately equal to d^2y/dx^2 which is:-

$$\frac{d^2y}{dx^2} = n(n+1) \alpha x^{n-1}$$

In terms of the thickness:-

$$\frac{d^2y}{dx^2} = \frac{t}{2} (n+1)^{(2n+1)/n} x^{n-1}$$

Thus with $n > 1$ the curvature increases from zero at $x = 0$, (the trailing edge), to a maximum at $x = 1$. Thus these sections are flat near the trailing edge. The higher derivatives up to the m^{th} ,

where/

where $n \leq n+1$, are also zero at $x = 0$. Thus the extent of the flat portion increases with n . The length marked "Flat" in Figs. 1, 2, is that over which the value of y differs from αx , (or, for $n < 1$, from $\alpha(1-x)$), by less than 1% of the semi-thickness $t/2$.

For $n = 1$, the curvature is constant and equal to $4t$. For $n < 1$ the curvature is infinite at $x = 0$ and decreases to a minimum at $x = 1$. For $n = 0$ the radius of curvature is approximately proportional to the distance from the leading edge.

3.4 Bump sections : effect of tilting

The sections have a property which makes them particularly useful for testing as "bumps" on the wall of a wind tunnel. This is that, if the section is tilted about its trailing edge through a small angle, the result is a similar section with a different thickness to chord ratio.

Consider the section $y = \alpha_1 x(1-x^n)$. The effect of tilting this through a small angle α_2 about the origin is approximately to add an ordinate $\alpha_2 x$. Thus the section becomes

$$\begin{aligned} y &= \alpha_1 x(1-x^n) + \alpha_2 x \\ &= (\alpha_1 + \alpha_2)x \left[1 - \frac{\alpha_1}{(\alpha_1 + \alpha_2)} x^n \right] \end{aligned}$$

Hence,

$$\frac{y}{c} = (\alpha_1 + \alpha_2) \frac{x}{c} \left[1 - \left(\frac{x}{c} \right)^n \right]$$

where

$$c = \left(\frac{\alpha_1 + \alpha_2}{\alpha_1} \right)^{1/n}$$

The result is a similar section with a chord increased by the factor $\left(\frac{\alpha_1 + \alpha_2}{\alpha_1} \right)^{1/n}$, and the thickness/chord ratio increased by the factor $\frac{\alpha_1 + \alpha_2}{\alpha_1}$.

Thus if α_2/α_1 is small, the increase of chord is about $1/n$ times the increase in thickness ratio. So if n is fairly large, greater than 2, say, the thickness ratio of the bump may be varied by tilting it, with only slight variation of the chord.

4. Round Noses

4.1 Properties required

A geometrical method is required for rounding the leading edge of any sharp-nosed aerofoil section. The resulting section should have the following properties:-*

1./

*The suitability of a particular nose radius or nose shape depends on its effect on the aerodynamic characteristics of the section, which must be determined by experiment or by calculation of the pressure distribution. The geometrical properties given are not an adequate guide to suitable nose shapes.

1. It should be possible to vary the nose radius independently of the shape of the basic section.
2. Near the leading edge the curve should approximate to an ellipse or hyperbola, whatever the shape of the basic section.
3. The curve should be a smooth one and the curvature should decrease monotonically from the leading edge.
4. Subject to 3, the length cut off the sharp-nosed section should be as small as possible relative to the nose radius.
5. The curve should fair in rapidly to the basic section.

The last two properties, 4 and 5, are not always necessary, but they are desirable when a family of aerofoils is required, differing from one another only near the nose.

There are many ways of obtaining these properties. One fairly simple method is given below.

4.2 The function $\tanh \sqrt{\beta \left[\frac{x^2}{a^2} - 1 \right]}$

Suppose $y = \pm \eta(x)$ is the ordinate of a symmetrical sharp-nosed aerofoil section with its leading edge at $x = 0$. Consider the equation:-

$$y = \pm \eta \tanh \sqrt{\beta \left[\frac{x^2}{a^2} - 1 \right]} \quad \dots(4.1)$$

This is a section with a round nose, with a radius and shape depending on a and β , which for suitable values of these parameters has the properties stated above. Fig. 6 illustrates the parameters involved.

From equation (4.1), $y = 0$ when $x = a$. Thus the length cut off in rounding the nose is a . For x very close to a , η is approximately equal to its value η_a at a , and $\tanh \sqrt{\beta \left[\frac{x^2}{a^2} - 1 \right]}$ is approximately equal to $\sqrt{\beta \left[\frac{x^2}{a^2} - 1 \right]}$. Hence near $x = a$, y is approximately given by:-

$$y_1 = \pm \eta_a \sqrt{\beta \left[\frac{x^2}{a^2} - 1 \right]}$$

or,
$$\frac{x^2}{a^2} - \frac{y_1^2}{(\eta_a \sqrt{\beta})^2} = 1$$

The curve is thus approximately a hyperbola with axes a and $\eta_a \sqrt{\beta}$. The nose radius, ρ , is the value of $y \frac{dy}{dx}$ at $x = a$, which is:-

$$\rho = y \frac{dy}{dx} = \beta \eta_a^2 \cdot \frac{x}{a^2}$$

$$\rho = \beta \frac{\eta_a^2}{a}$$

This value for the nose radius is exact, as may be seen by differentiating the exact expression for y .

4.3 Second approximation to the leading-edge shape

Let $x = a(1+\epsilon)$. The previous section shows that for $\epsilon \ll 1$, the nose shape approximates to a hyperbola. Now consider values of ϵ such that ϵ^2 , but not ϵ , is negligible.

To this approximation,

$$\eta = \eta_a + a\epsilon\psi,$$

where ψ is the value of $d\eta/dx$ at $x = a$. The second approximation to $\tanh \theta$ for small θ is $\frac{\tanh \theta}{\theta} = 1 - \frac{\theta^2}{3}$.

Hence,

$$\begin{aligned} \tanh \sqrt{\beta \left[\frac{x^2}{a^2} - 1 \right]} &= \left(1 - \frac{\beta}{3} \left[\frac{x^2}{a^2} - 1 \right] \right) \sqrt{\beta \left[\frac{x^2}{a^2} - 1 \right]}, \\ &\approx \left(1 - \frac{2\beta\epsilon}{3} \right) \sqrt{\beta \epsilon (2+\epsilon)}. \end{aligned}$$

Hence the second approximation to y is given by:-

$$y_a = \pm \eta_a \left(1 + \frac{a\psi\epsilon}{\eta_a} \right) \left(1 - \frac{2\beta\epsilon}{3} \right) \sqrt{\beta \epsilon (2+\epsilon)},$$

or,
$$y_a^2 = 2\eta_a^2\beta\epsilon \left[1 + \epsilon \left(\frac{1}{2} + \frac{2a\psi}{\eta_a} - \frac{4\beta}{3} \right) \right]. \quad \dots(4.2)$$

Consider a conic section with the same leading-edge radius $\beta \frac{\eta_a^2}{a}$, and let the ratio of its axes be N . Then its semi-axes are $\frac{a}{N\beta \frac{\eta_a^2}{a}}$ in the y direction and $N^2\beta \frac{\eta_a^2}{a}$ in the x direction. Hence the equation of the conic is:-

$$y_c^2 + \frac{\left(x - a - N^2\beta \frac{\eta_a^2}{a} \right)^2}{N^2} = \frac{N^2\beta^2 \eta_a^4}{a^2},$$

or,
$$y_c^2 = 2(x-a) \beta \frac{\eta_a^2}{a} - \frac{(x-a)^2}{N^2},$$

or,
$$y_c^2 = 2\eta_a^2\beta\epsilon \left[1 - \frac{1}{2} \frac{a^2\epsilon}{\beta\eta_a^2 N^2} \right]. \quad \dots(4.3)$$

So, /

So, comparing equations (4.2) and (4.3), the aerofoil section and the conic coincide, to this approximation, if:-

$$\frac{1}{2} + \frac{2a\psi}{\eta_a} - \frac{4\beta}{3} = -\frac{1}{2} \frac{a^2}{\beta\eta_a^2 N^2},$$

or, putting $\frac{\eta_a}{a} = \phi$,

$$\beta^2 - \frac{3}{8} \beta \left[1 + \frac{4\psi}{\phi} \right] - \frac{3}{8N^2 \phi^2} = 0. \quad \dots(4.4)$$

For $N^2 < 0$ the conic is a hyperbola. For $N = \infty$ it is a parabola, and the condition for this is $\beta = \frac{3}{8} \left(1 + \frac{4\psi}{\phi} \right)$. For $N^2 > 1$ the conic is an ellipse with its major axis on the x-axis, and hence with its greatest curvature at the leading edge. For $N^2 = 1$ the conic is a circle of radius $\beta \frac{\eta_a^2}{a}$. For $0 < N^2 < 1$ the conic is an ellipse with its minor axis on the x-axis. Its curvature thus increases with y, and this violates condition 3 of Section 4.1.

Thus condition 3, that the curvature should decrease monotonically from the leading edge, will not be satisfied unless $1/N^2 < 1$. The present paper will give no proof that the condition is satisfied if $1/N^2 < 1$, for any particular section shape, but will suggest that, for normal section shapes, this appears likely to be a good criterion.

4.4 Effects of β for a linear basic section

Suppose the basic section is linear, or approximately linear for $x < 2a$, say. Then $\phi = \psi$ and $\eta = \phi x$. Equation (4.4) becomes:-

$$\beta^2 - \frac{15}{8} \beta - \frac{3}{8N^2 \phi^2} = 0.$$

A graph of β against ϕ for $N = 1$, the limiting value for which the nose shape approximates a circle, is shown in Fig. 7.

The effect of β on the nose shape for different values of ϕ and ψ is given by equation (4.4) but this is rather difficult to visualize. A parameter which seems to be useful in practice is the ratio to the nose radius of the ordinate at a+p of the basic section. Denoting this ordinate by η_{a+p} , the parameter γ is:-

$$\begin{aligned} \gamma &= \frac{\eta_{a+p}}{\rho}, \\ &= \frac{\eta_a}{\rho} + \psi, \\ &= \frac{a}{\beta\eta_a} + \psi, \\ &= \frac{1}{\beta\phi} + \psi. \end{aligned} \quad \dots(4.5)$$

Hence, /

Hence,

$$\beta = \frac{1}{\phi(\gamma-\psi)} .$$

For the linear section, for which $\psi = \phi$,

$$\gamma = \frac{1}{\beta\phi} + \phi .$$

Hence

$$\beta = \frac{1}{\phi(\gamma-\phi)} .$$

Fig. 7 shows β plotted against ϕ for values of γ of 1.0, $\sqrt{2}$ and 2.0. The curve for $\gamma = \sqrt{2}$ differs little from that for $N = 1$. Fig. 8 shows the variation of γ with ϕ for $N = 1$. The curve has a minimum at $\phi = 0.5$, and the variation of γ over the useful range of ϕ is from about 1.3 to 1.6.

Fig. 9 shows, for $\phi = 0.1, 0.2$ and 0.4 , the effect of γ on the nose shapes. The curves drawn are those with $\gamma = 1, \sqrt{2}$ and 2 . With $\gamma = 1$ the curvature clearly increases away from the nose, the nose shapes have "shoulders" and are unacceptable. With $\gamma = 2$ the curvature clearly decreases monotonically away from the nose, and the curves are geometrically acceptable nose shapes. With $\gamma = \sqrt{2}$ the curves appear to follow the circle of curvature at the leading edge through a large angle. The nose shapes still appear acceptable, although it is not clear from the figure whether the curvature is a maximum at the leading edge. Fig. 8 shows that in fact N is greater than unity for $\phi = 0.4$, about equal to unity for $\phi = 0.2$, and less than unity for $\phi = 0.1$.

Thus the value of γ gives a useful criterion as to whether the nose shape is acceptable. It should not be less than the value given by Fig. 8, for $N = 1$. This value gives a curve which probably will have a monotonically decreasing curvature. The curvature appears to fall very suddenly where the curve departs from the nose circle, however, and a rather better nose shape may be obtained by choosing a value of γ greater than this by a factor of $\sqrt{2}$.

Fig. 10 shows the variation of N with γ for three values of ϕ . For $\gamma = 2$, N equals 1.42 at $\phi = 0.1$, passes through infinity as ϕ increases and equals $2.18\sqrt{-1}$ at $\phi = 0.4$. The appearance of the curves of Fig. 9, with γ constant and equal to 2.0 suggests that, so long as $N > 1$, a constant value of γ gives curves of generally similar appearance, and γ may therefore be a more practical parameter than N .

4.5 Effects of non-linearity of the basic section

The effect of non-linearity of the basic section is to alter the ratio ψ/ϕ in equation (4.4). Usually the basic section is convex and $\psi < \phi$.

Fig. 11 shows, for various values of β ($=\beta_1$) when $\psi/\phi = 1$, the change in β which is required to keep $N\phi$ constant when ψ/ϕ differs from unity. The method of using this figure is to determine the value of β which, for the existing ϕ , would give a suitable N for $\psi/\phi = 1$. Then from the figure, obtain the correction to be subtracted from this value of β for the actual value of ψ/ϕ .

The/

The effect of ψ/ϕ on γ , or on the value of β required for a given γ , may be obtained from equation (4.5). The effect on γ is considerably smaller than the effect on N , unless ϕ/γ is unusually large.

4.6 Fairing of the nose shape into the basic section

For large θ , $\tanh \theta$ is approximately equal to $1-2e^{-2\theta}$. Hence for sufficiently large x/a , the curve

$$y = \pm \eta \tanh \sqrt{\beta \left[\frac{x^2}{a^2} - 1 \right]},$$

is approximately given by

$$y = \pm \eta \left[1 - 2e^{-2\sqrt{\beta \left[\frac{x^2}{a^2} - 1 \right]}} \right].$$

Thus the curve is exponentially asymptotic to the basic section. Fig. 12 shows, plotted against β , the values of x/a for which

$\frac{\eta-y}{\eta} = 0.01, 0.001$ and 0.0001 . This shows that even for low values of β

the ordinate is within 1% of the basic section at a distance less than $2a$ from the leading edge ($x = a$). The curve is very rapidly asymptotic, as is required.

4.7 Application of the round noses to unsymmetrical sections

In order to preserve the symmetry of the nose, and to place the leading edge on the centre line of the basic section, and not on the x -axis, the semi-thickness of the basic section, and this only, must be

multiplied by $\tanh \sqrt{\beta \left[\frac{x^2}{a^2} - 1 \right]}$. Thus if the upper surface is $\eta_u(x)$ and the lower surface $\eta_L(x)$, the equation of the round-nosed section is:-

$$y = \frac{1}{2}(\eta_u + \eta_L) \pm \frac{1}{2}(\eta_u - \eta_L) \tanh \sqrt{\beta \left[\frac{x^2}{a^2} - 1 \right]}.$$

The nose shape is then similar to that produced by rounding the nose of a symmetrical basic section with an ordinate equal to the semi-thickness, $\frac{1}{2}(\eta_u - \eta_L)$.

4.8 Application of the round noses to the aerofoils of Section 3, and comparison with the RAE 100-104 sections²

The noses may clearly be applied to any of the sections with $n > 0$. The more useful range is $n \geq 1$, for which $x = 0$ at the trailing edge. The equation of the round-nosed aerofoils is then:-

$$y = \pm a x (1-x^n) \tanh \sqrt{\beta \left[\frac{(1-x)^2}{a^2} - 1 \right]}.$$

For/

For small values of a , ϕ and ψ are given approximately by:-

$$\phi = n \alpha \left[1 - \frac{(n+1)}{2} a \right]$$

$$\psi = n \alpha \left[1 - (n+1) a \right]$$

Hence

$$\frac{\psi}{\phi} = 1 - \frac{(n+1)}{2} a$$

Fig. 4c shows the section $n = 6$, $a = 0.0133$, compared with the RAE 100². The two sections have the same maximum thickness position and are similar except that the $n = 6$ section has a slightly smaller trailing-edge angle, and a leading-edge radius about half that of the RAE section. Thus it is possible, by suitable choice of n and a , to produce curves which are similar to the RAE sections but with any desired leading-edge radius. It is also possible to produce sections with the same maximum thickness position and leading-edge radius as the RAE sections: these are thus curves given by explicit equations which, except in detail, are similar to the RAE sections.

As an example of this, a curve has been designed to fit the RAE 101 section as closely as possible. with $\alpha = 0.0906$, $n = 3.90$, $a = 0.040$ and $\beta = 1.71$, the nose radius, maximum thickness position and trailing-edge angle are the same as for the 10% thick RAE 101 and the ordinates are everywhere the same to within 2% of the maximum ordinate.

The RAE sections have certain disadvantages at high speeds due to the fact that the curvature has a maximum just ahead of the flat tail section. The curves described above do not have this disadvantage.

5. Droop-Nosed and Cambered Sections

5.1 Camber

The aerofoils of Section 3 may, of course, be cambered by the addition of any suitable camber line. Mr. H. H. Pearcey has suggested that the ordinates of the same section, or of another member of the family, might form a useful camber line. Then the section would become:-

$$y = \alpha_1 x(1-x^{n_1}) \pm \alpha_2 x(1-x^{n_2}) \quad \dots(5.1)$$

The round nosed sections would be:-

$$y = \alpha_1 x(1-x^{n_1}) \pm \alpha_2 x(1-x^{n_2}) \tanh \sqrt{\beta \left[\frac{(1-x)^2}{a^2} - 1 \right]}$$

assuming $n_2 > 1$ so that $x = 0$ at the trailing edge. The thickness of the sharp-nosed section, from equation (3.3), would be $2\alpha_2 \left(\frac{1}{n_2+1} \right)^{1/n_2} \frac{n_2}{n_2+1}$,

while its camber would be $\alpha_1 \left(\frac{1}{n_1+1} \right)^{1/n_1} \frac{n_1}{n_1+1}$.

5.2 Nose droop

A curve is required having an extended and drooped leading edge, faired in to the basic section of equation (3.1), or the cambered section of equation (5.1). A suitable curve is shown in Fig. 13. The upper surface, (A, Fig. 13), except near the rounded nose, is simply the basic section, equation (3.1) or (5.1), extended to values of x greater than unity. The lower surface at the rear (B) is also that of the basic section, equation (3.1) or (5.1). Near the nose a fairing curve (C) joins this section to a straight line (D). This, and the upper surface, fair into the rounded nose (E).

The equations of the different curves making up the section are as follows:-

$$\begin{aligned}
 \text{(A)} \quad y &= \alpha_1 x(1-x^{n_1}) + \alpha_2 x(1-x^{n_2}) &= A \\
 \text{(B)} \quad y &= \alpha_1 x(1-x^{n_1}) - \alpha_2 x(1-x^{n_2}) &= B \\
 \text{(C)} \quad y &= -L \log (e^{-B/L} + e^{-D/L}) &= C \\
 \text{(D)} \quad y &= -m(x-b) &= D \\
 \text{(E)} \quad y &= \frac{A+D}{2} \pm \frac{(A-D)}{2} \tanh \sqrt{\beta \left[\frac{(c-x)^2}{a^2} - 1 \right]} &= E, \dots(5.2)
 \end{aligned}$$

where c is given by $A = D$, or:-

$$\alpha_1 c(1-c^{n_1}) + \alpha_2 c(1-c^{n_2}) + m(c-b) = 0 \quad \dots(5.3)$$

The assumption that the curve may be treated as a set of five separate parts is normally justified, owing to the rapidity of the convergence of C and E to D. It may not be justified if $c-a-1$ is small, or negative. If this assumption is not justified, D must be replaced by C in the equations for E and c. This gives the exact equation for the curve which is:-

$$y = \frac{A+C}{2} \pm \frac{(A-C)}{2} \tanh \sqrt{\beta \left[\frac{(c-x)^2}{a^2} - 1 \right]}, \quad \dots(5.4)$$

where c is given by:-

$$\alpha_1 c(1-c^{n_1}) + \alpha_2 c(1-c^{n_2}) = -L \log \left\{ e^{-\frac{1}{L}[\alpha_1 c(1-c^{n_1}) - \alpha_2 c(1-c^{n_2})]} + e^{-\frac{m}{L}(x-b)} \right\} .$$

The approximate value for c given by equation (5.3) will, however, almost always be sufficiently accurate, even when the approximation $C = D$ in equation (5.2) is not justifiable.

5.3 Effects of the parameters

The complete equation (5.4) contains nine independent parameters. These may be listed as follows:-

<u>Parameter</u>	<u>Effect</u>
n_1	Position of maximum ordinate of the camber line (see Sections 3.1, 5.1)
n_2	Maximum thickness position of the basic section (see Section 3.1)
α_1	Camber of the aerofoil, (see Sections 3.2 and 5.1)
α_2	Thickness of the aerofoil, (see Section 3.2)
m	Slope of the linear portion under the nose (Fig. 13)
b	Intersection of the linear portion with the y-axis (Fig. 13)
L	Extent of fairing between the linear portion and the rear under-surface, (see below)
a	Length cut off the leading edge in rounding the nose (Section 4.2 and Fig. 13)
β	Leading edge radius and nose shape (Section 4)
c	Chord of the sharp-nosed section (Fig. 13). Not independent but determined by $n_1, n_2,$ α_1, α_2, m and b .

The only parameter whose effect is not clear from preceding sections or from Fig. 13 is L , which affects the fairing C , Fig. 13.

Consider two curves $y = \eta_1(x)$ and $y = \eta_2(x)$, Fig. 14, which cross one another at $x = x_0$, where $\eta_1 = \eta_2 = \eta_0$, and such that $\eta_2 > \eta_1$ for $x > x_0$ and $\eta_2 < \eta_1$ for $x < x_0$. Then the curve:-

$$y = L \log [e^{\eta_1/L} + e^{\eta_2/L}] , \quad \dots(5.5)$$

is a smooth curve which is exponentially asymptotic to η_1 for $x < x_0$ and to η_2 for $x > x_0$. Its value at $x = x_0$ is

$$\begin{aligned} y &= L \log 2 e^{\eta_0/L} \\ &= \eta_0 + L \log 2 \\ &= \eta_0 + 0.693 L . \end{aligned}$$

Equation (5.5)/

Equation (5.5) may be rearranged as:-

$$\frac{y-\eta_1}{L} = \log \left[1 + e^{\frac{\eta_2-\eta_1}{L}} \right], \quad \dots(5.6)$$

or as

$$\frac{y-\eta_2}{L} = \log \left[1 + e^{\frac{\eta_1-\eta_2}{L}} \right].$$

Fig. 15 shows a graph of $\frac{y-\eta_1}{L}$ against $\frac{\eta_2-\eta_1}{L}$. This shows that the difference between y and η_2 or η_1 becomes very small when $\frac{\eta_2-\eta_1}{L}$ or $\frac{\eta_1-\eta_2}{L}$ exceeds about 3 or 4. When $e^{\frac{\eta_2-\eta_1}{L}}$ is small, equation (5.6) becomes approximately:-

$$y = \eta_1 + L e^{\frac{\eta_2-\eta_1}{L}}.$$

Similarly when $e^{\frac{\eta_1-\eta_2}{L}}$ is small,

$$y = \eta_2 + L e^{\frac{\eta_1-\eta_2}{L}}.$$

Thus the curve is exponentially asymptotic to η_1 and η_2 . y differs from η_2 by less than $0.01 L$ for $\eta_2-\eta_1 > 4.605 L$, and by less than $0.001 L$ for $\eta_2-\eta_1 > 6.908 L$.

This method may be used to produce a fairing between any two suitable intersecting curves. When applied to the curves B and D of Section 5.2 and Fig. 13 the fairing curve C results.

This method clearly could be used to produce a round nose by fairing the upper and lower surfaces of a sharp-nosed aerofoil. The result would give a shape similar to one of the curves of Section 4, but for a very low, and invariable, value of β . Thus the method is not very practical for this purpose.

References/

References

<u>No.</u>	<u>Authors</u>	<u>Title, etc.</u>
1	R. Michel, F. Marchaud and J. Le Gallo	Influence de la position du maître- couple sur les écoulements transsoniques autour de profils à pointes. O.N.E.R.A. Publication No.72, (1954).
2	R. C. Pankhurst and H. B. Squire	Calculated pressure distributions for the RAE 100-104 aerofoil sections. R.A.E. Tech. Note Aero.2039.

JMT

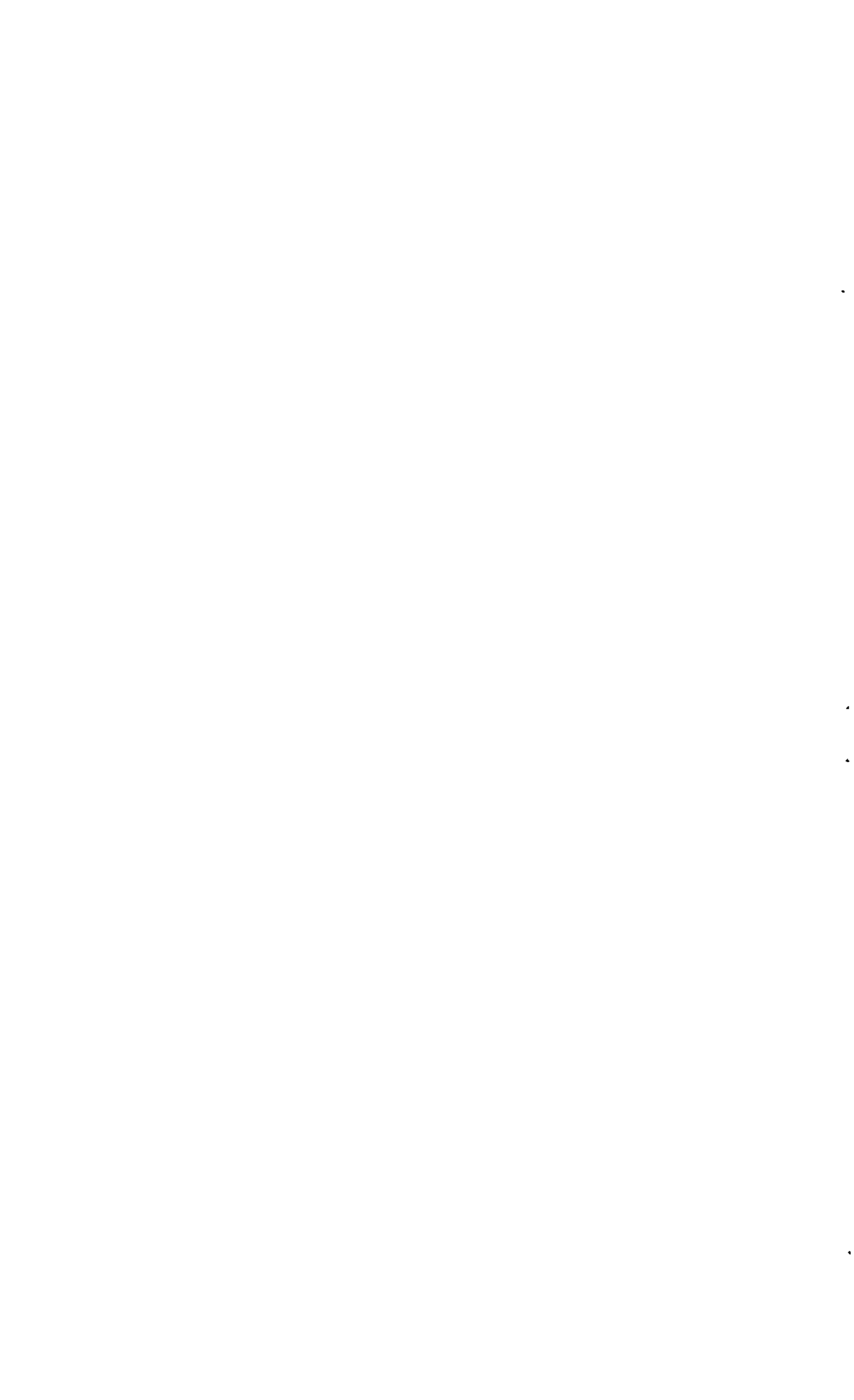
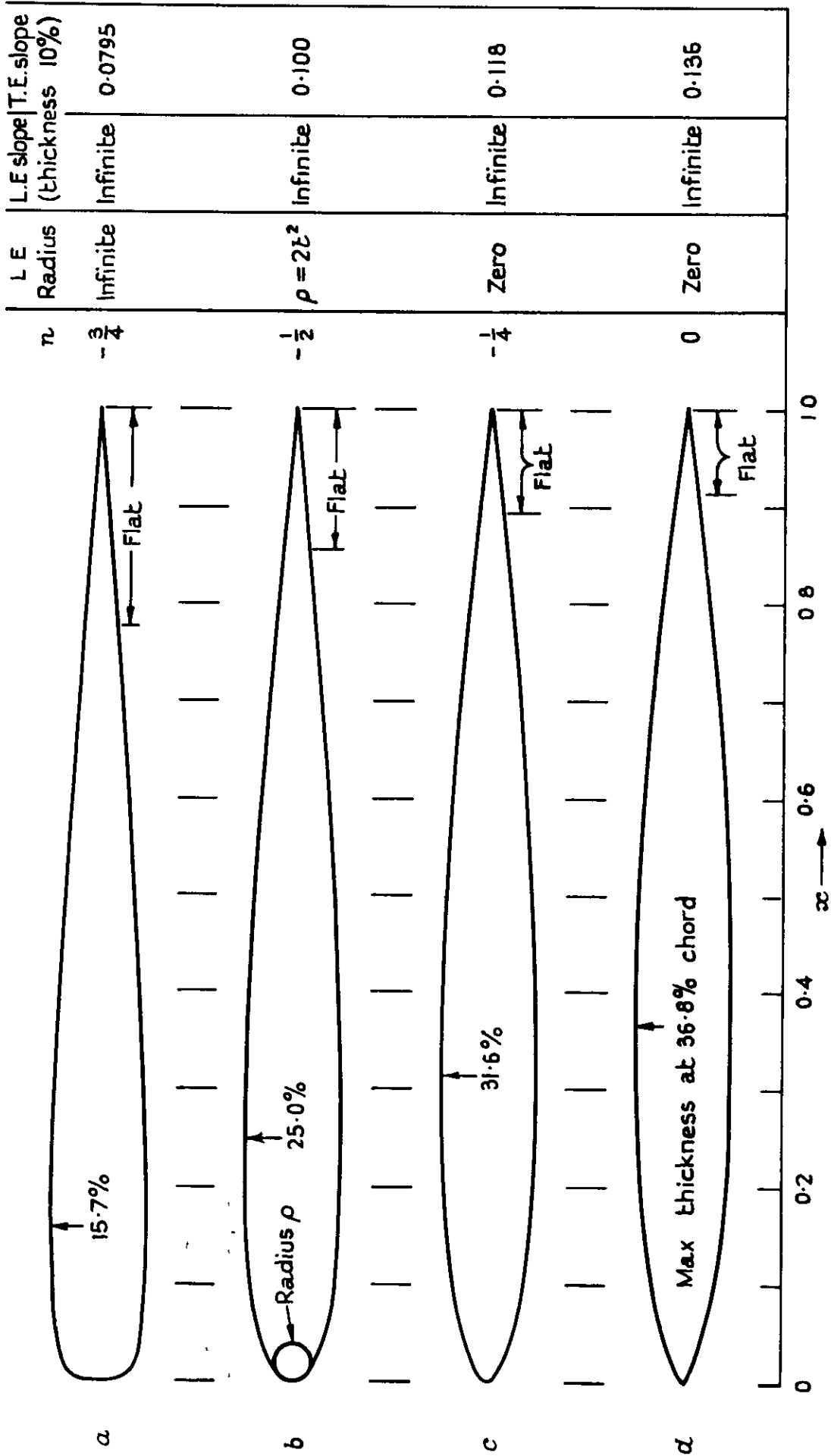


FIG. 1.



Examples of the curves $y = \pm \alpha x(1-x^2)$ for 10% thick sections ($t = 0.10$)

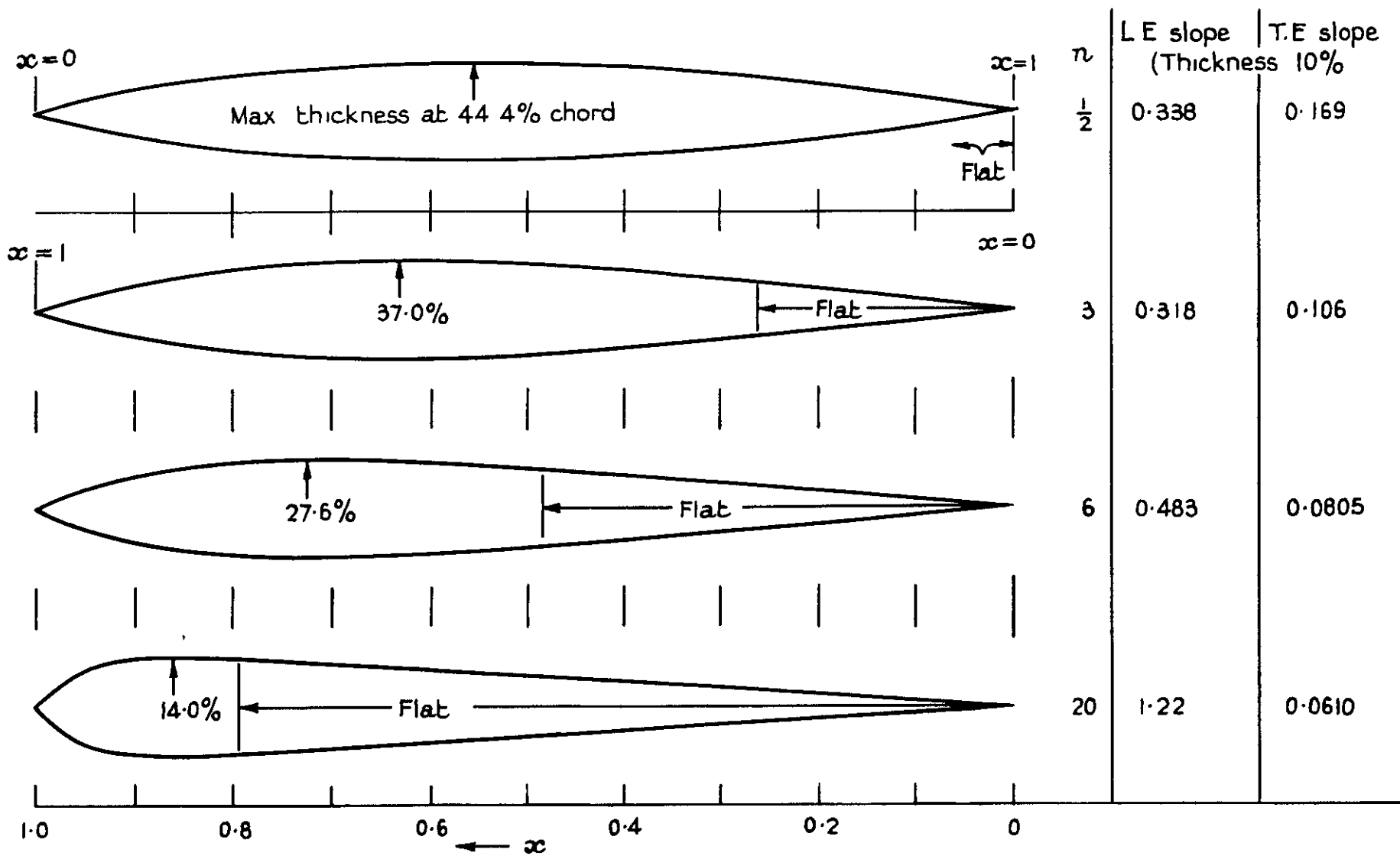
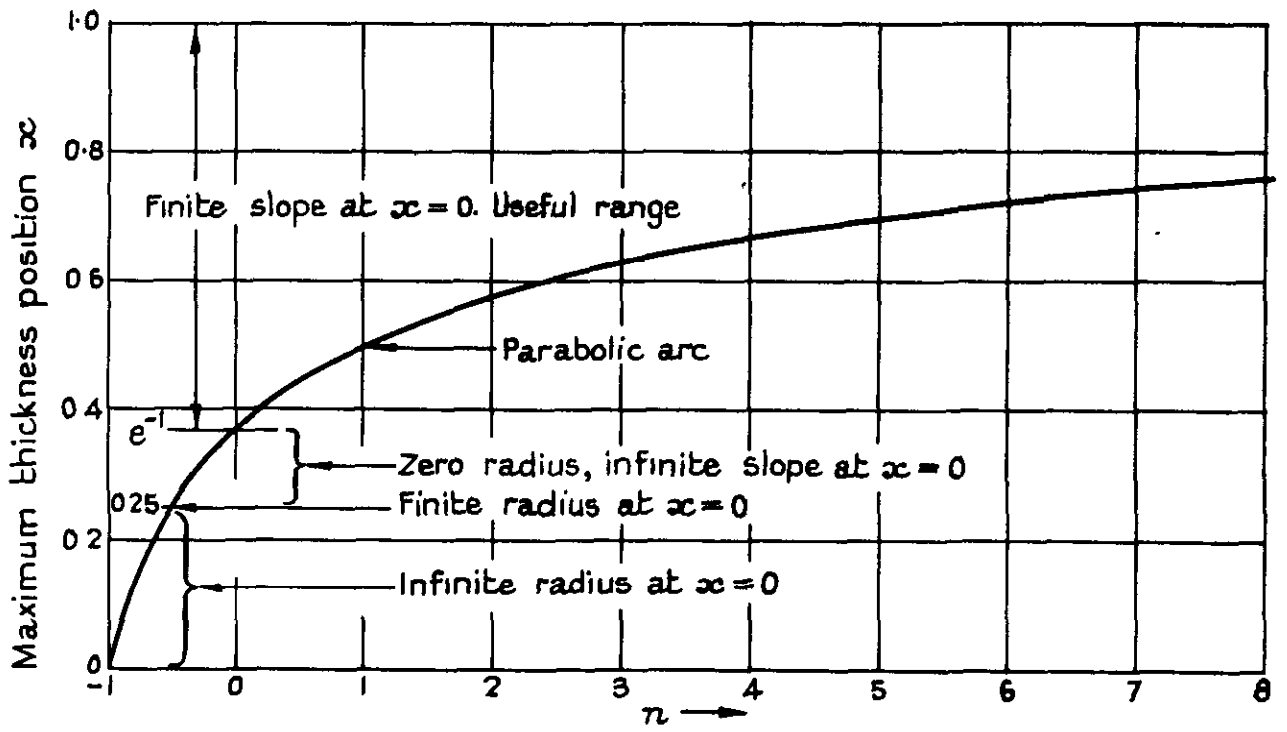


FIG. 2.

Examples of the curves $y = \pm \alpha x (1 - x^n)$ for 10% thick sections ($t = 0.10$)

Fig. 3.4



Maximum thickness position of $y = ax(1 - x^n)$

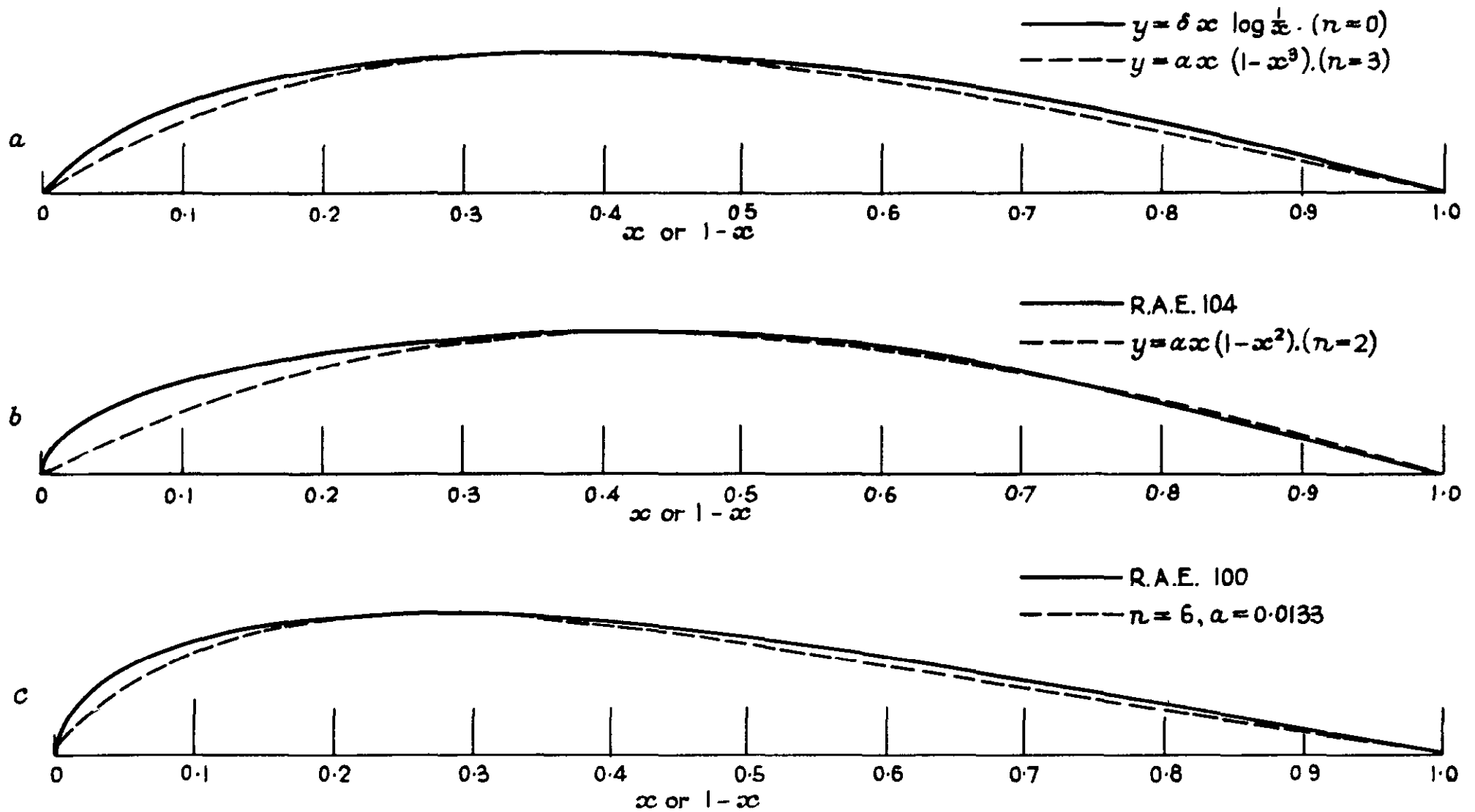
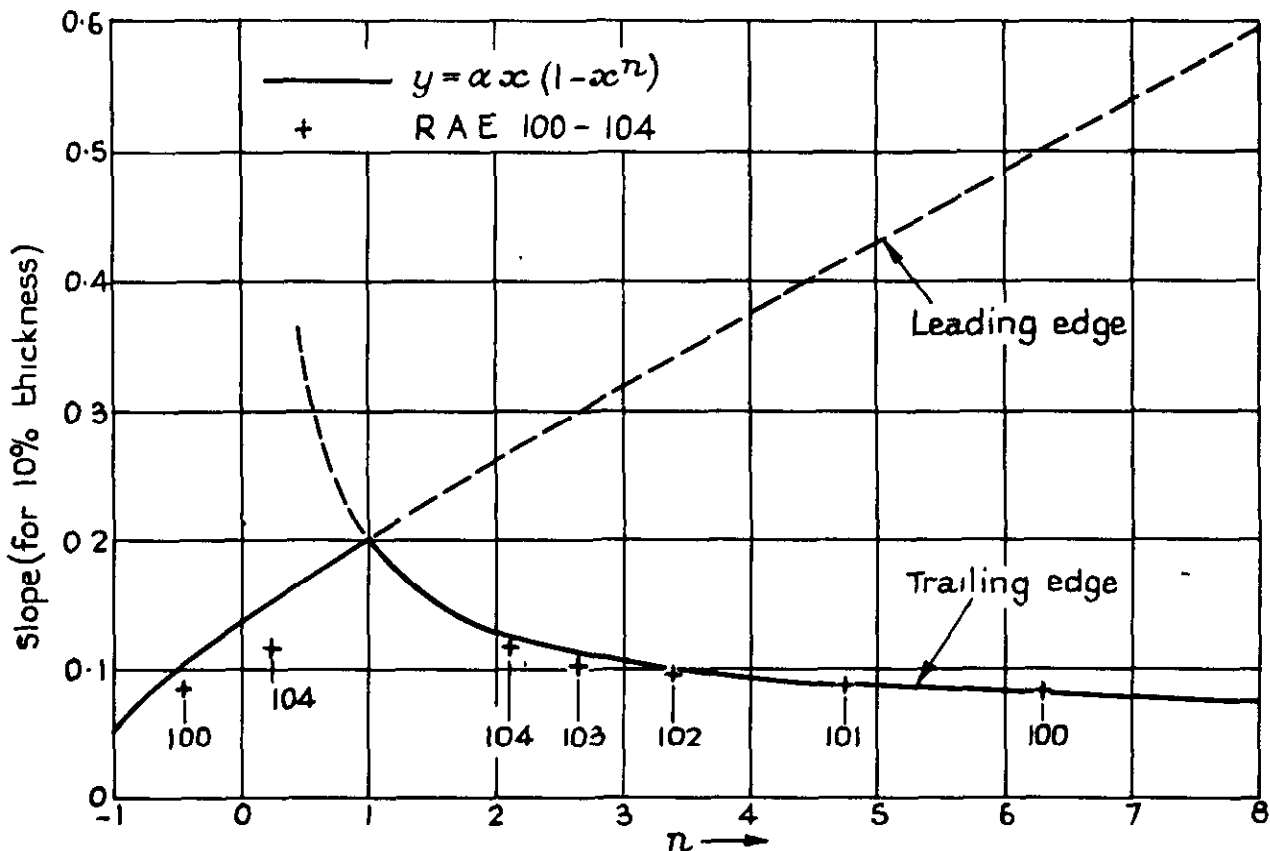


FIG. 4.

Comparisons between aerofoil sections

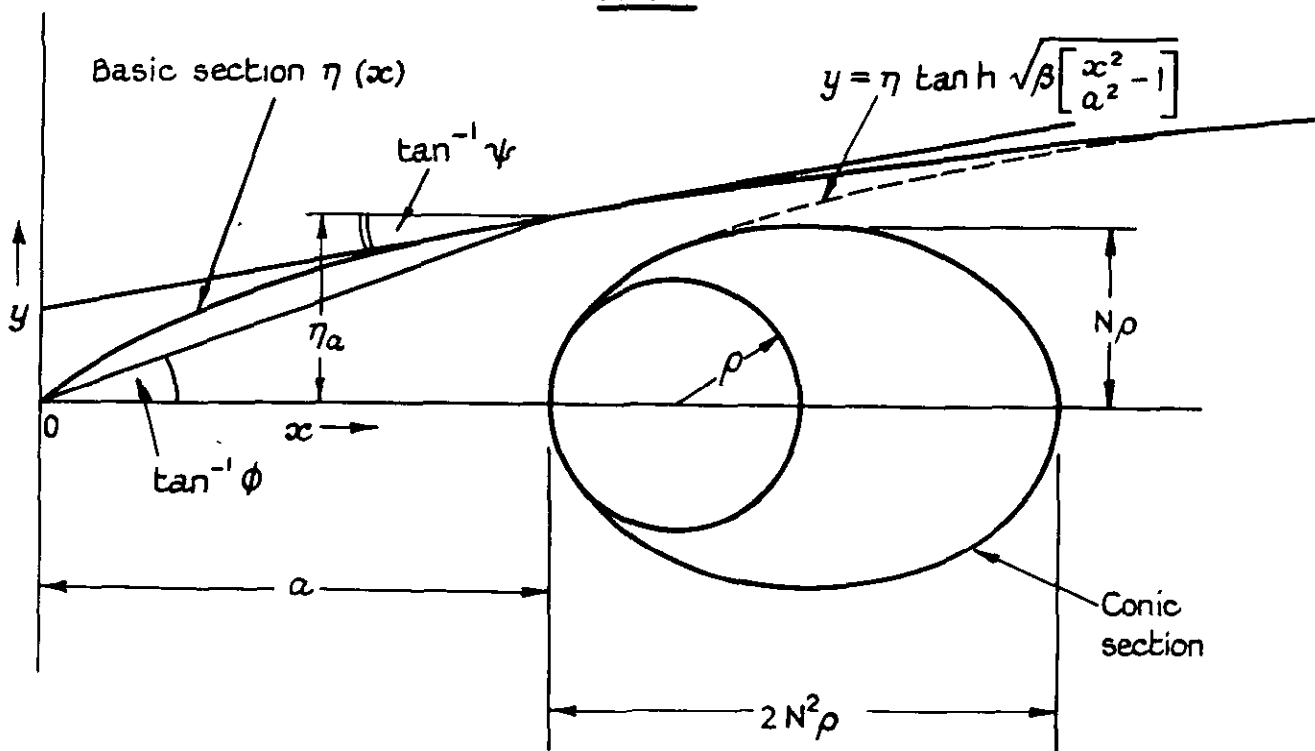
FIGS. 5 & 6

FIG. 5.



Graph of leading and trailing edge slopes of sections $\alpha x (1 - x^n)$ against n

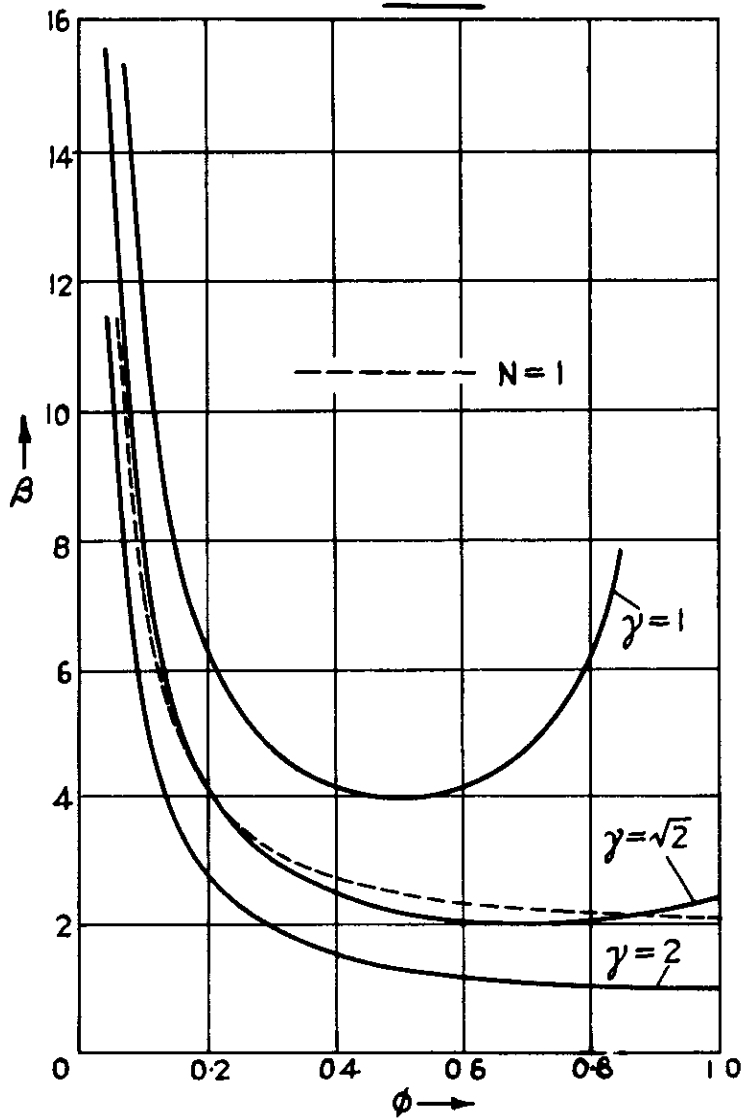
FIG. 6.



Method of producing round noses, showing the parameters involved

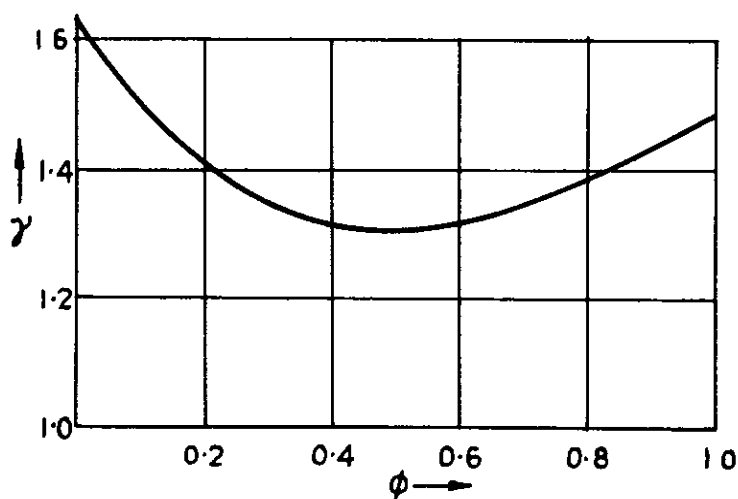
FIGS. 7 & 8.

FIG 7.



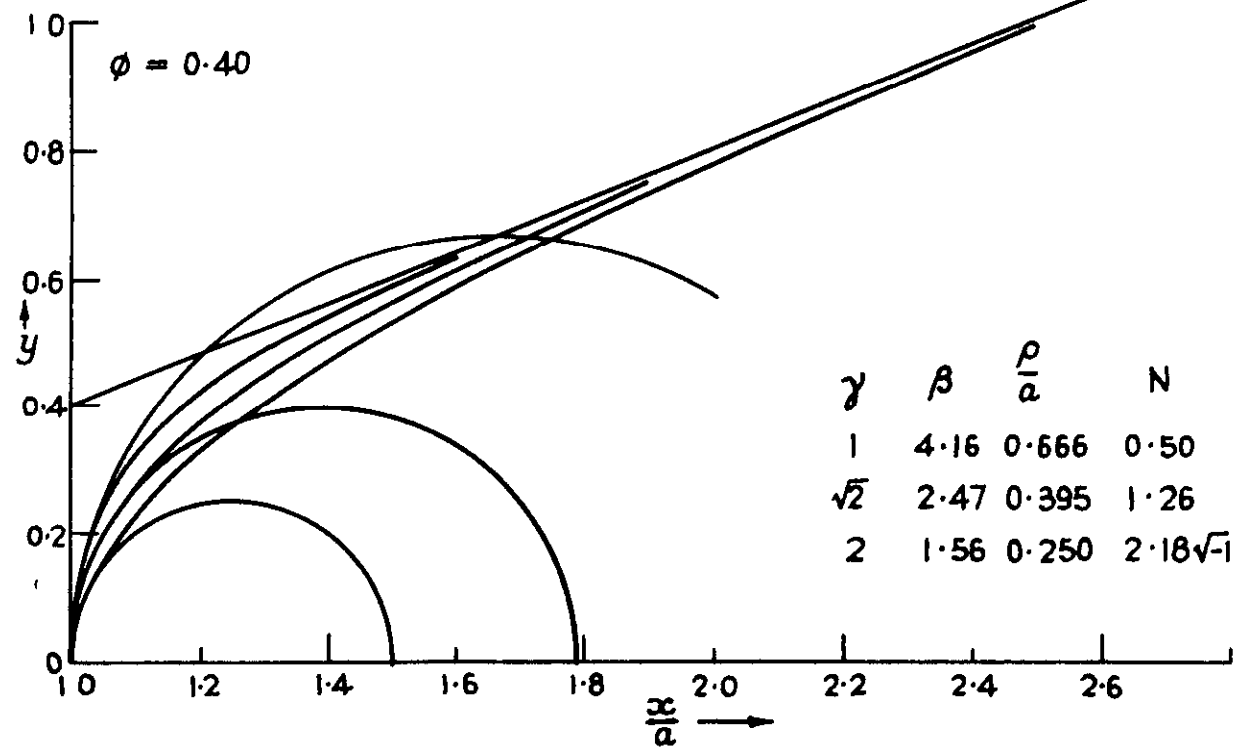
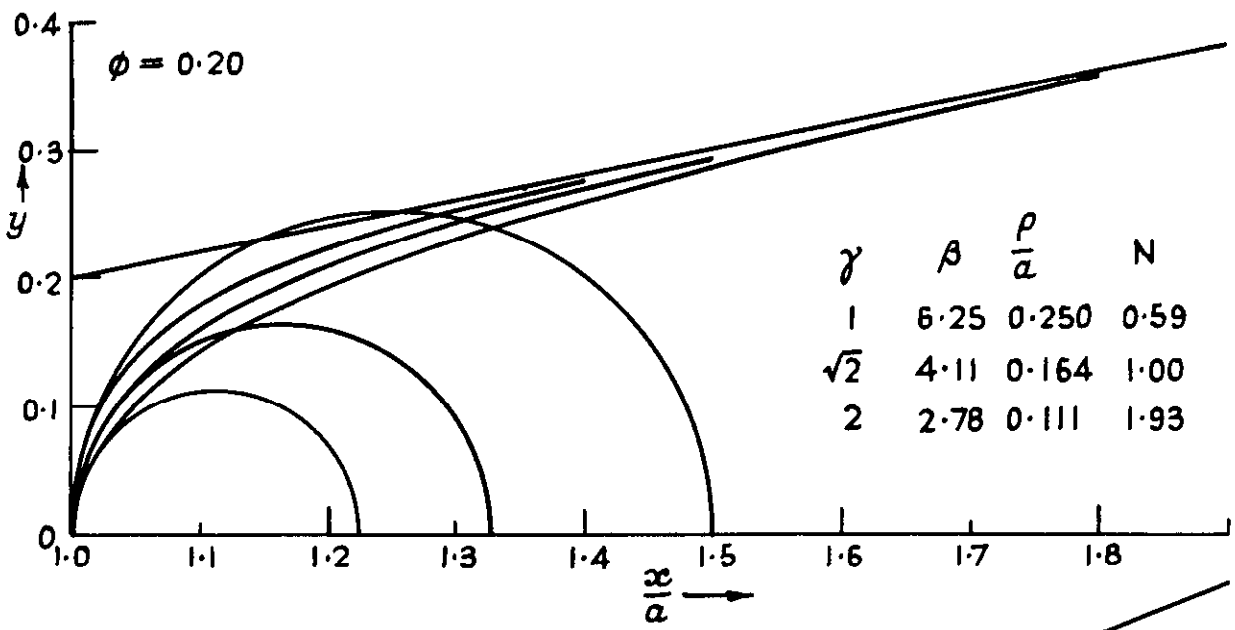
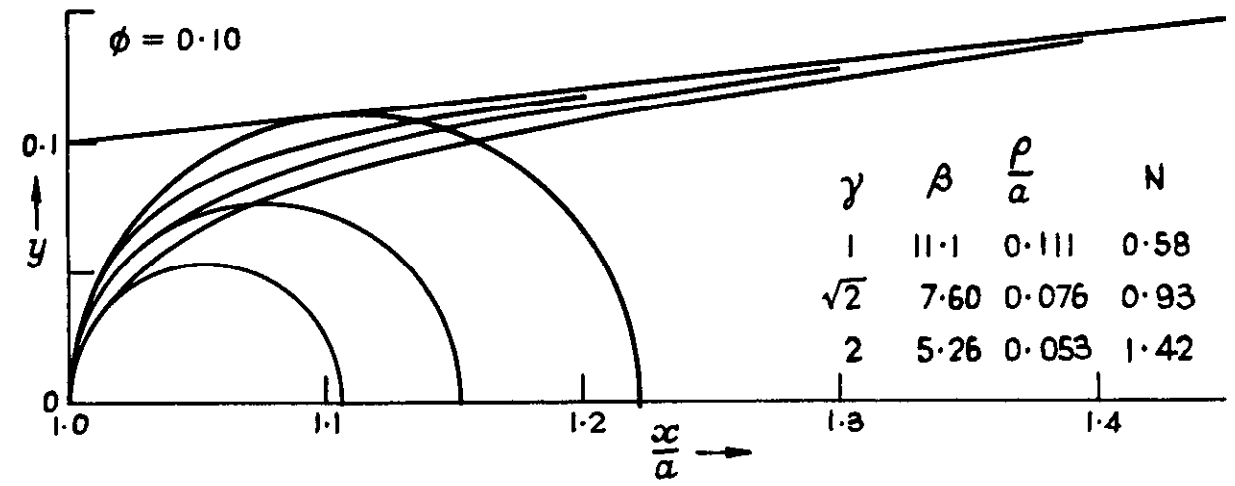
Graph of β against ϕ . (β should not exceed the value giving $N=1$)

FIG. 8.



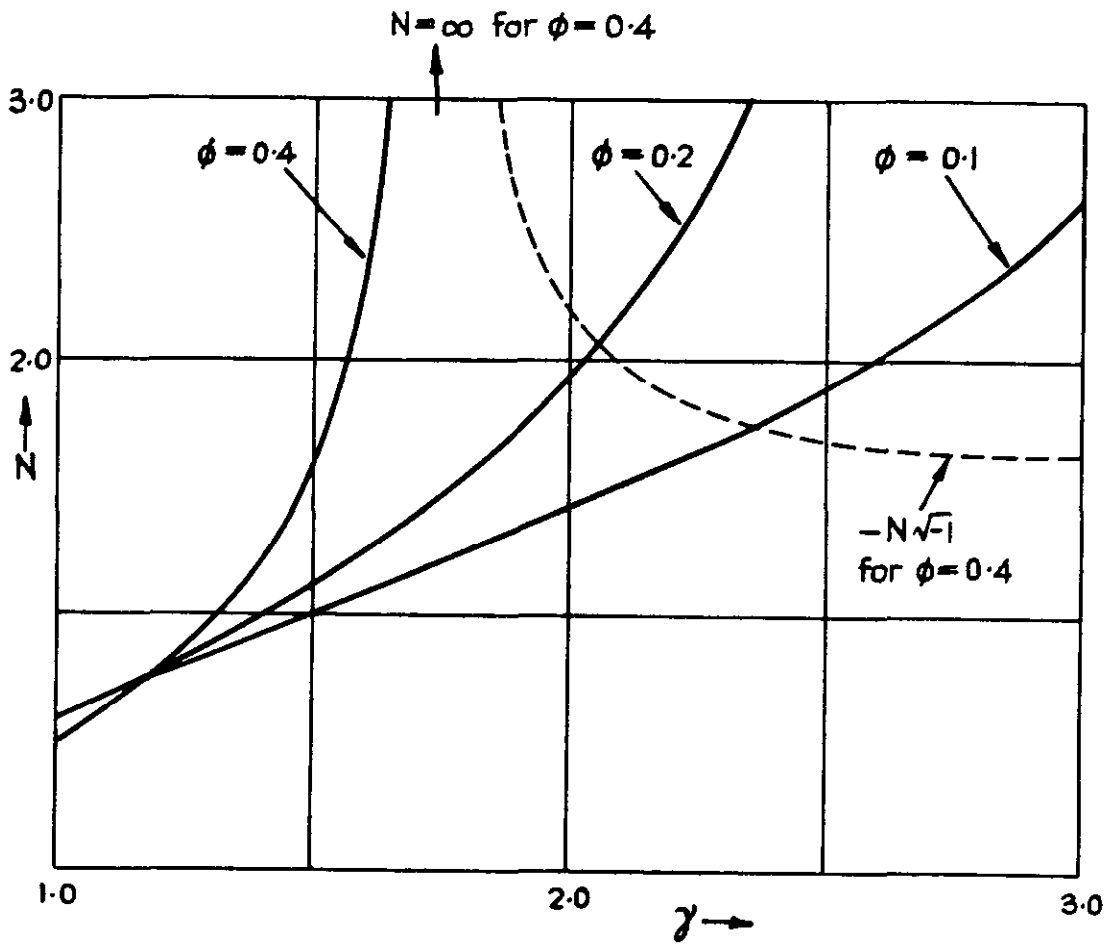
Graph of γ against ϕ for $N=1$. (γ should not be less than the value giving $N=1$)

FIG. 9.



Nose shapes: effect of ϕ and γ .

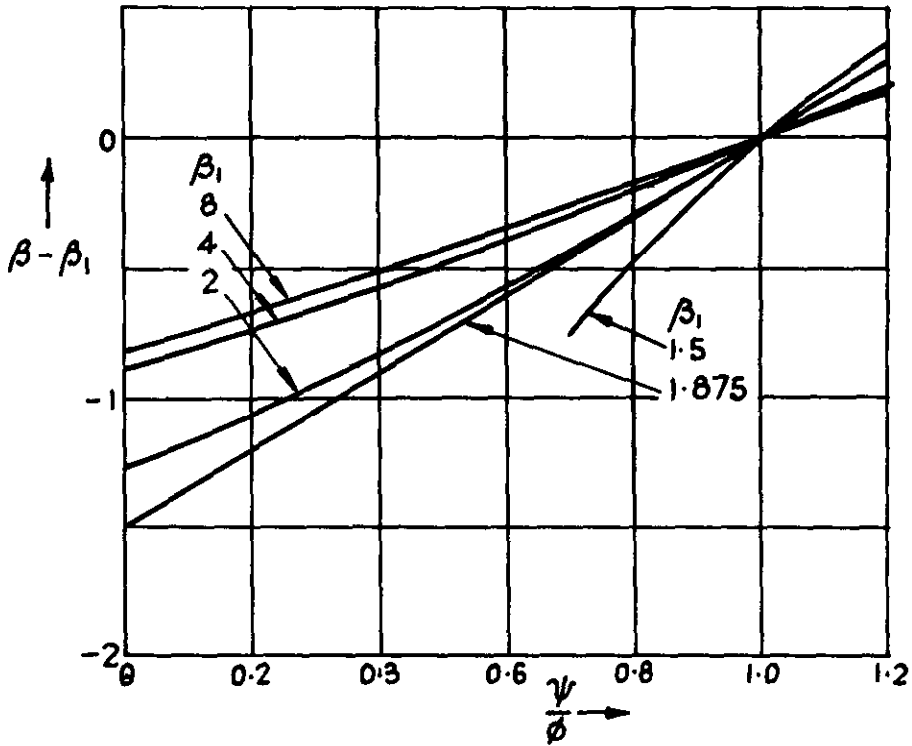
FIG. 10.



Graph of N against γ for three values of ϕ

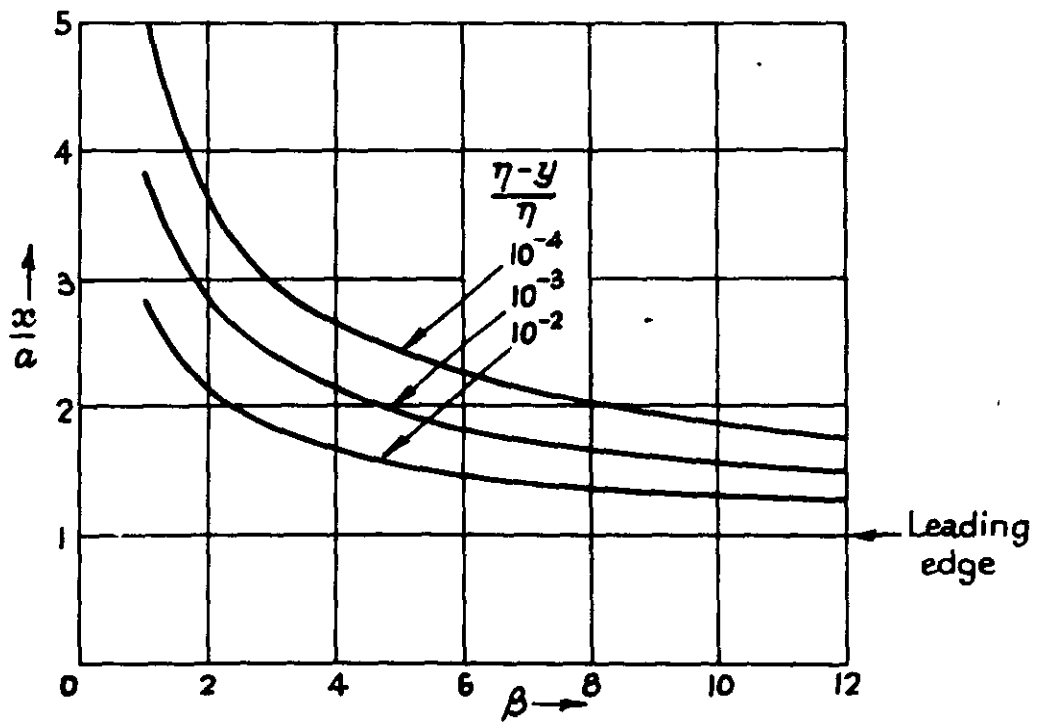
FIGS. 11 & 12

FIG. 11



Effect of $\frac{\psi}{\phi}$ on β for constant $N\phi$

FIG. 12.



Graphs of $\frac{x}{a}$ against β for $\frac{\eta-y}{\eta} = 10^{-2}, 10^{-3}$ and 10^{-4}

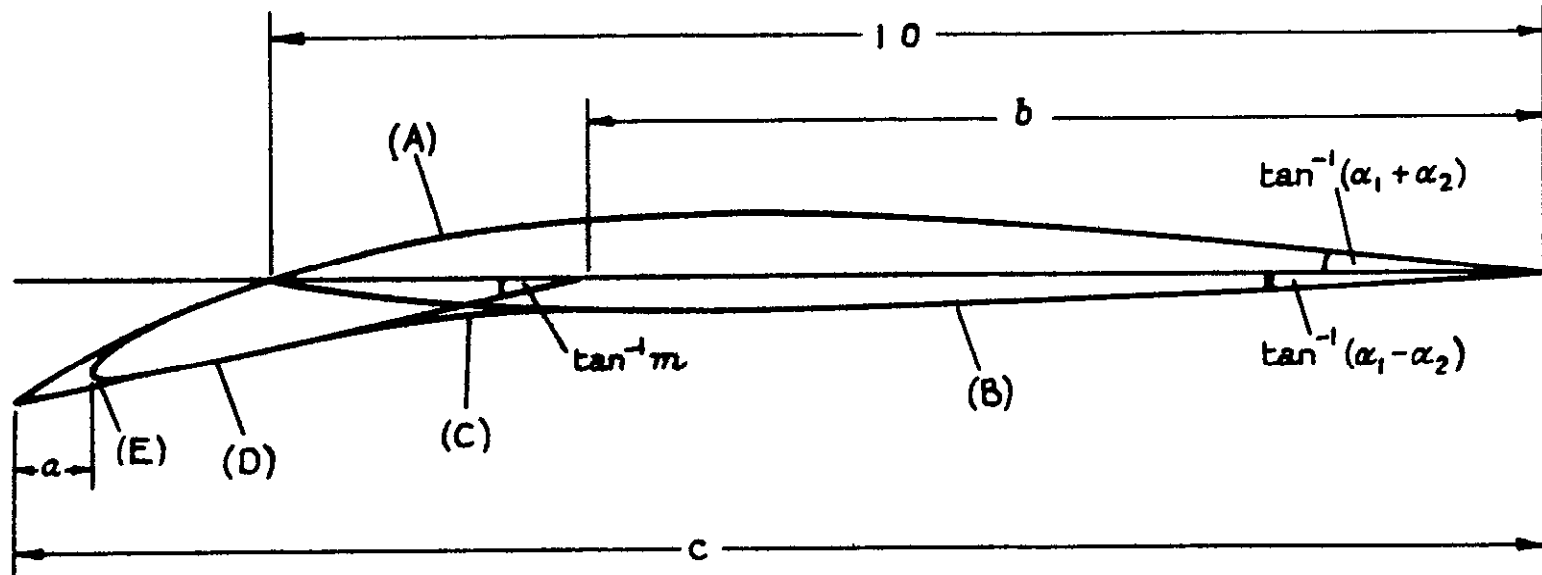
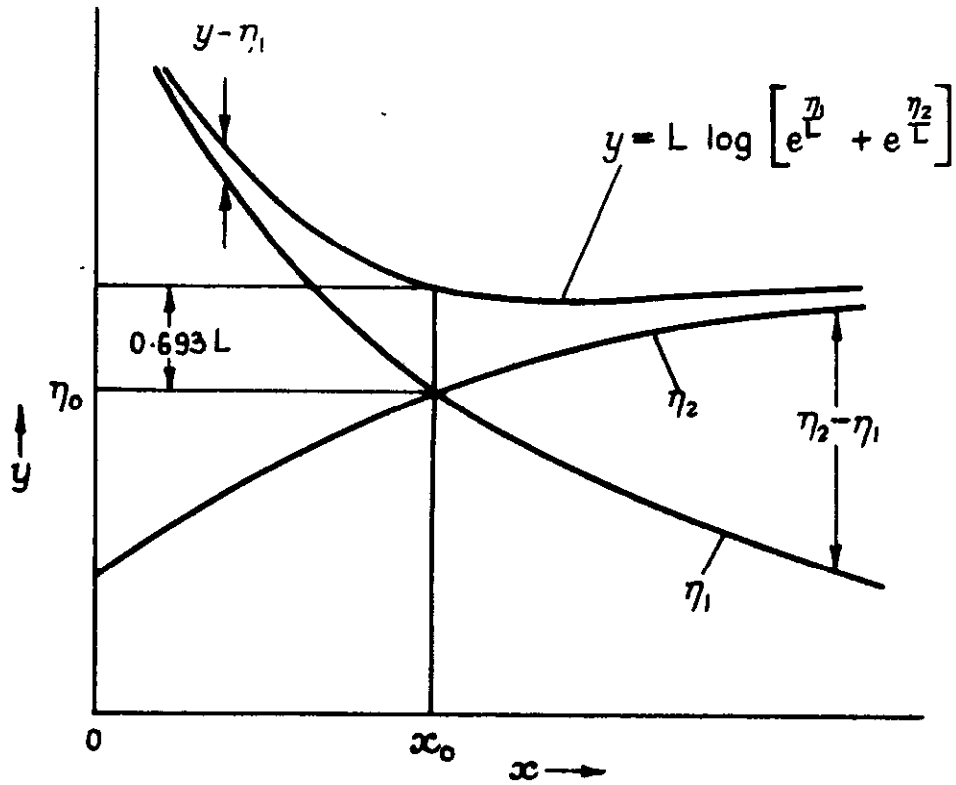


Fig. 13

Round-nosed aerofoil with droop, showing the effects of some of the parameters.

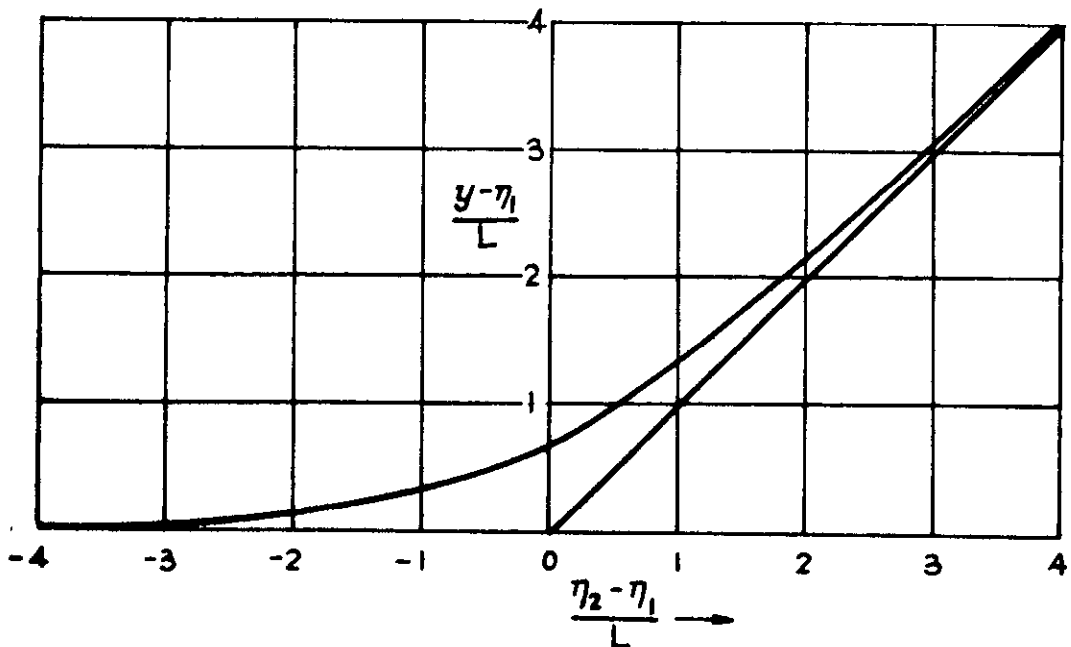
FIG. 14 & 15.

FIG. 14.



Method of fairing two intersecting curves.

FIG. 15.



Graph of $\frac{y - \eta_1}{L}$ against $\frac{\eta_2 - \eta_1}{L}$

C.P. No. 358

(19,054)

A.R.C. Technical Report

Crown copyright reserved

Printed and published by
HER MAJESTY'S STATIONERY OFFICE

To be purchased from
York House, Kingsway, London W.C. 2
423 Oxford Street, London W.1
13A Castle Street, Edinburgh 2
109 St Mary Street, Cardiff
39 King Street, Manchester 2
Tower Lane, Bristol 1
2 Edmund Street, Birmingham 3
80 Chichester Street, Belfast
or through any bookseller

Printed in Great Britain

S O Code No. 23-9010-58

C.P. No. 358